

# Optical properties of Er-doped GaN

H. Castañeda López

*Instituto Mexicano del Petróleo, Mexico.*

Seong-Il Kim, Young-Hwan Kim, and Yong Tae Kim

*Semiconductor Devices Laboratory, KIST,*

*Seoul 136-791, Korea.*

Akihiro Wakahara

*Department of Electrical and Electronic Engineering, Toyohashi University of Technology,*

*Toyohashi 441-8580, Japan.*

Chang-Sik Son

*Department of Photonics, FIMM,*

*Silla University, Busan 617-736, Korea,*

*e-mail: csson@silla.ac.kr*

In-Hoon Choi

*Department of Materials Science and Engineering, Korea University,*

*Seoul 136-701, Korea.*

Recibido el 9 de junio de 2006; aceptado el 11 de septiembre de 2006

Optical properties of Er (Erbium)-doped GaN epilayers have been investigated using photoluminescence (PL). Various doses of Er ions were implanted on GaN epilayers by ion implantation. Sharp visible green emission lines due to inner 4f shell transitions for Er<sup>3+</sup> were observed from the PL spectrum of Er-implanted GaN. The emission spectrum consists of two narrow green lines at 537 and 558 nm. The green emission lines are identified as Er<sup>3+</sup> transitions from the <sup>5</sup>H<sub>11/2</sub> and <sup>4</sup>S<sub>3/2</sub> levels to the <sup>4</sup>I<sub>15/2</sub> ground state. The stronger peaks in the  $5 \times 10^{14} \text{ cm}^{-2}$  sample, together with the relatively higher intensity of the Er<sup>3+</sup> luminescence in the lower doped sample, imply that some damage remains in the  $1 \times 10^{15} \text{ cm}^{-2}$  sample. The peak positions of emission lines due to inner 4f shell transitions for Er<sup>3+</sup> do not change with increasing temperature. This indicates that Er<sup>3+</sup> related emission depends very little on the ambient temperature.

**Keywords:** GaN; implantation; Er; photoluminescence.

Las propiedades ópticas de epícapas de GaN dopadas con Er (erbium) se han investigado usando fotoluminiscencia (FL). Varias dosis de iones de Er se implantaron en epícapas de GaN por implantación de iones. Se observaron líneas claramente visibles de emisión verde debidas a la transición de la capa interna 4f para Er<sup>3+</sup> del espectro de FL de GaN implantado con Er. El espectro de emisión consiste en dos líneas verdes delgadas a 537 y 558 nm. Las líneas de emisión verdes se identifican como transiciones del Er<sup>3+</sup> de los niveles 5H11/12 y 4S3/2 al estado base 4I15/2; los picos más fuertes en la muestra de  $5 \times 10^{14} \text{ cm}^{-2}$ , junto con la intensidad relativamente más alta de la luminescencia Er<sup>3+</sup> en la muestra dopada inferior. Esto implica que aún permanece algún daño en la muestra de  $1 \times 10^{15} \text{ cm}^{-2}$ . Las posiciones pico de las líneas de emisión debidas a las transiciones internas 4f para Er<sup>3+</sup> no cambian con la temperatura creciente. Esto indica que la emisión relacionada con Er<sup>3+</sup> depende muy poco de la temperatura del ambiente.

**Descriptores:** GaN; implantación; Er; fotoluminiscencia.

PACS: 78.55.-m

## 1. Introduction

Rare earth (RE) materials such as Er (Erbium), Eu (Europium), Tm (Thulium), and Pr (Praseodymium) have been of considerable interest for possible applications in light emitting devices and for their unique optical properties [1-6]. The rare earth luminescence is reported as it depends very little on the nature of the host and the ambient temperature.

GaN is one of the promising materials for optoelectronic devices in the short wavelength region, because of its wide band-gap and high level of optical activity even under conditions of rather high defect density. In order to obtain an efficient optical device, improvement of the luminescence capability is important. RE-doped GaN has been of great interest for application in display and light emitting devices. The

emission from a RE-GaN is spectrally sharp and requires no color filtering since it arises from atomic RE transition. Recently, many results have been reported concerning the optical properties of Er-, Eu-, Tm-, and Pr-doped GaN grown on sapphire or Si [1-6].

Er is known to be an efficient activator in several hosts, giving rise to strong green luminescence. The development of green-emission devices by GaN-based semiconductors is attractive from the viewpoint of a monolithic device composed of red, green, and blue light emitting diodes. Ion implantation is widely used to incorporate impurity atoms into the semiconductors and have become a workhorse technology in modern semiconductor device fabrication. A high concentration of dopant atoms can be formed in localized regions of a semiconductor host [7-9].

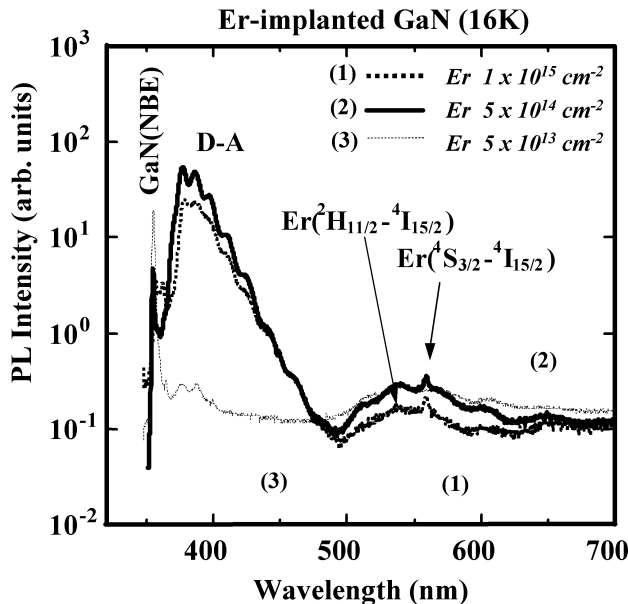


FIGURE 1. PL spectrum of Er-doped GaN at 16 K. Er ions were implanted at three different doses of  $5 \times 10^{13}$ ,  $5 \times 10^{14}$ , and  $1 \times 10^{15} \text{ cm}^{-2}$  at room temperature.

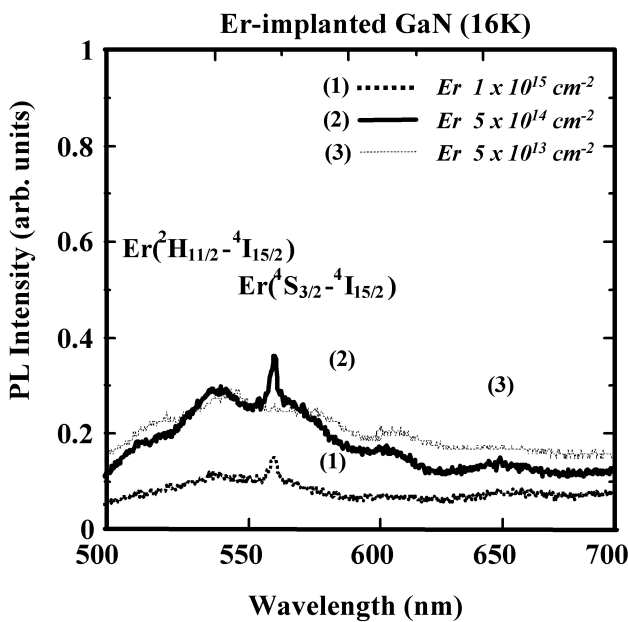


FIGURE 2. The higher resolution PL spectrum from Er-doped GaN of Fig. 1.

In this work, we have reported the optical characteristics of the photoluminescence (PL) spectrum of Er-doped GaN grown by metalorganic chemical vapor deposition (MOCVD) on sapphire. We have observed sharp green visible emission from Er ions in GaN epilayers. PL properties of Er-doped GaN with various conditions for ion implantation have been investigated. Er ions are introduced onto GaN epilayers grown on (0001) sapphire substrates by ion implantation.

## 2. Experiments

We have fabricated an Er-doped GaN structure by ion implantation on the GaN epilayers grown by MOCVD. The doping of GaN with Er can be carried out by MOCVD and molecular beam epitaxy (MBE), both during growth. And it can also be done by ion implantation after growth.

GaN on sapphire epilayers grown by MOCVD were implanted with 200 keV Er ions at three different doses of  $5 \times 10^{13}$ ,  $5 \times 10^{14}$ , and  $1 \times 10^{15} \text{ cm}^{-2}$  at room temperature. It was chosen to give an approximation of a square concentration implant profile in the GaN epilayer (the projected range and peak concentration were  $\sim 40 \text{ nm}$  and  $\sim 3.1 \times 10^{19} \text{ cm}^{-3}$ , respectively.) Following implantation, the samples were annealed at  $1050^\circ\text{C}$  for 30 minutes in 33%  $\text{NH}_3$  diluted with  $\text{N}_2$  to repair damage resulting from the Er implantation and to avoid decomposition of nitrides. The PL spectra were measured at 16 K using a He-Cd (325 nm) laser.

## 3. Results and discussion

Figure 1 shows the PL spectra of Er doped GaN for three different doses of  $5 \times 10^{13}$ ,  $5 \times 10^{14}$  and  $1 \times 10^{15} \text{ cm}^{-2}$ , measured at 16 K. After the thermal annealing for 30 min, sharp peaks of visible emission were obtained from Er-doped GaN thin films. Photo excitation by a He-Cd (325 nm), which is above the GaN band-gap, resulted in relatively sharp green emission. RE ions can be excited by an energy transfer process from electron-hole pairs generated in conduction and valance bands (by photons from a He-Cd laser). The luminescence of Er was excited indirectly, generating electron-hole pairs in GaN hosts by He-Cd laser. By using the high excitation optical energy source above the GaN band-gap, the transition process can be more efficient. Because the electrons can be excited strongly from the valance to the conduction band, an efficient energy transfer to Er ions would be possible in GaN epilayers. We can see the band edge emission of Er doped GaN at around 400 nm and deep level emission around 500-600 nm.

Figure 2 shows the higher resolution PL spectrum of Fig. 1. It shows relatively sharp optical emissions due to 4f-4f electron transitions with energies largely independent of the dose density in Fig. 1. The strongest peak, at 558 nm, is due to the  $^4S_{3/2}$  levels for the  $^4I_{15/2}$  ground state transition and the other peak (537 nm) is identified as  $^5H_{11/2}$  levels for the  $^4I_{15/2}$  ground state transition. The optical emission and the PL peaks can be discussed easily by referring to Fig. 3, where the Er inner shell transition energies up to the GaN band gap energy (3.39 eV) are shown. Figure 3 shows the relevant energy levels in the PL spectrum of Er-doped GaN [10]. Optically active level energies are adjusted to reflect observed values in Er-implanted GaN. Sharp emission lines due to inner 4f shell transitions for  $\text{Er}^{3+}$  can be observed from the PL of Er-implanted GaN as shown in Figs. 1 and 2.

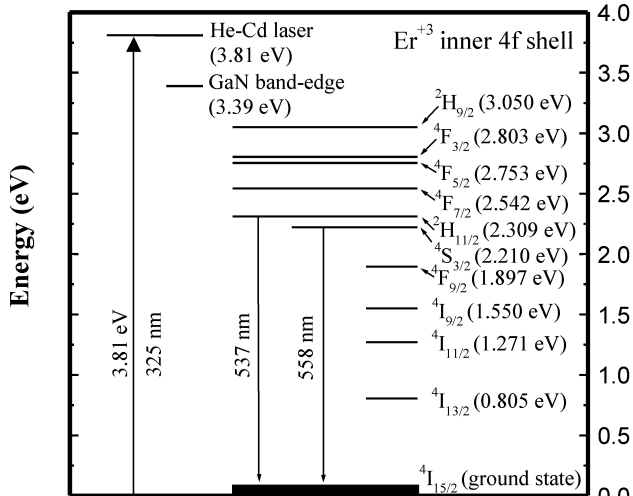


FIGURE 3. Relevant energy levels in the PL spectrum of Er-doped GaN.

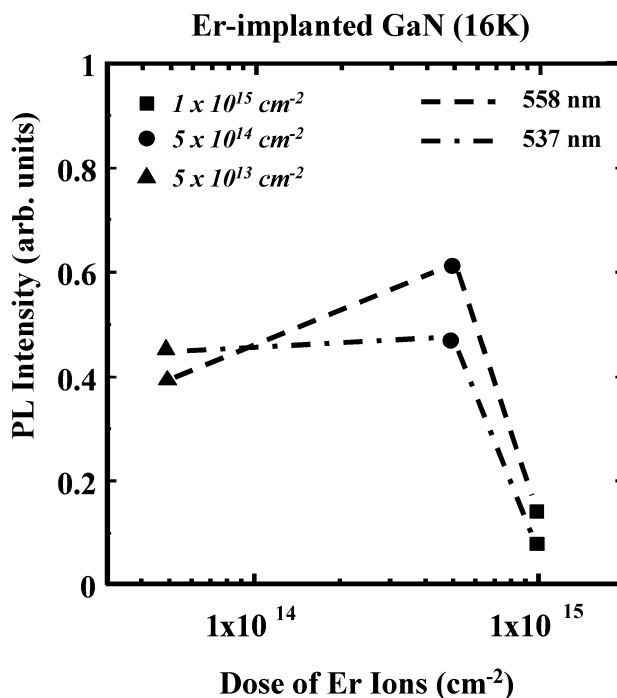


FIGURE 4. The intensity of the PL peaks of 537 nm and 558 nm as a function of the implanted dose density.

The narrow peaks may be caused by the energy transfer from the conduction band edge of GaN to tetra valent Er ions. It is expected that most of the excited carriers will be captured by the Er related isovalent traps. The excitation is carried out by a He-Cd laser source (325 nm). Many excited electrons pumped by a laser source experience nonradiative phonon transitions until they reach various inner shell energy levels of the Er atoms, where they can transfer their energy. The very important question is where the trivalent rare earth ions are incorporated in GaN: at substitutional sites on the metal sublattice and/or interstitial sites. After implantation, Er atoms occupy relaxed Ga substitutional sites. In this Ga

site the tetrahedral bonding for  $\text{Er}^{3+}$  results in the allowance of normally forbidden  $\text{Er}^{3+}$  inner-shell 4f-4f transitions. It is generally accepted that rare earth impurities in III-V semiconductors create isoelectronic traps [11]. But the RE ion in III-V semiconductors can occupy different sites (not only substitutional). They can create more complex centers involving other impurities or native defects.

Figure 4 shows the intensity of the PL peaks of 537 and 558 nm as a function of the implanted dose density. As the dose density is increased, the one peak intensity of 558 nm in the  $5 \times 10^{14} \text{ cm}^{-2}$  sample increased a little and that of 537 nm was nearly unchanged. But the two peaks in the  $1 \times 10^{15} \text{ cm}^{-2}$  sample decreased apparently compared to those of  $5 \times 10^{13} \text{ cm}^{-2}$  and  $5 \times 10^{14} \text{ cm}^{-2}$ . The stronger peaks in the  $5 \times 10^{14} \text{ cm}^{-2}$  sample, together with the relatively higher intensity of the  $\text{Er}^{3+}$  luminescence in the lower doped sample, indicate that some damage remains in the  $1 \times 10^{15} \text{ cm}^{-2}$  sample. In order to realize Er-GaN as a light emitting source, further improvement of the luminescence capability is required.

Figure 5 shows temperature dependence of PL intensity of Er-implanted GaN. With increasing temperature, the PL intensity of band edge emission rapidly decreases. In the case of the  $\text{Er}^{3+}$  related emission, the intensity does not much depend on the measured temperature. It implies that the capture rate of photon-generated carriers by  $\text{Er}^{3+}$  ions is not dependent on the temperature. The peak positions of emission lines due to inner 4f shell transitions for  $\text{Er}^{3+}$  do not change with an increasing temperature. These results indicate that  $\text{Er}^{3+}$  related emission depends very little on the ambient temperature.

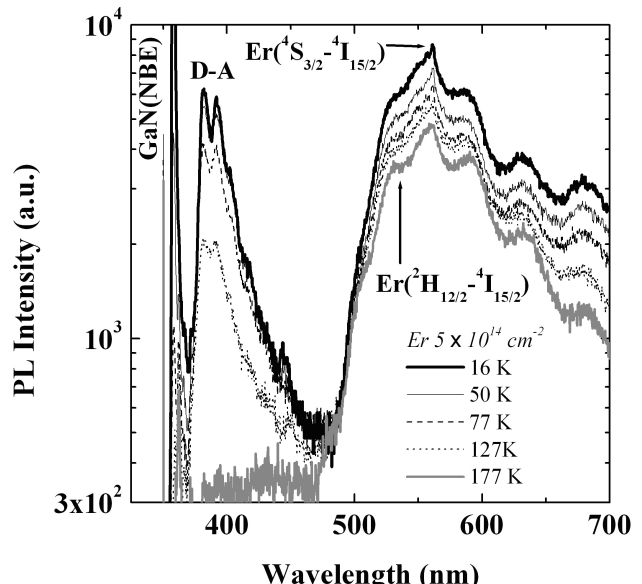


FIGURE 5. Temperature dependence of PL intensity of Er-implanted GaN.

#### 4. Conclusion

Visible light emission has been observed from Er-doped GaN epilayers. The GaN epilayers were grown by MOCVD on sapphire substrates and implanted with different doses of Er ions. The emission spectrum consists of two narrow peaks at 537 nm and 558 nm. The narrow lines have been identified as  $\text{Er}^{3+}$  transitions from the  $^5\text{H}_{11/2}$  and  $^4\text{S}_{3/2}$  levels to the  $^4\text{I}_{15/2}$  ground state. Some damage seems to have remained in the sample with the highest dose density of  $1 \times 10^{15} \text{ cm}^{-2}$ .

The peak positions of emission lines due to inner 4f shell transitions for  $\text{Er}^{3+}$  do not change with an increasing temperature. This indicates that  $\text{Er}^{3+}$  related emission depends very little on the ambient temperature.

#### Acknowledgement

This work is supported in part by International Science and Technology Cooperation Programs of KISTEP (M6-0302-01-0003/03-A01-03-003-10).

---

1. Z. Li, H. Bang, G. Piao, J. Sawahata, and K. Akimoto, *J. Crystal Growth* **240** (2002) 382.
2. D.S. Lee and A.J. Steckl, *Appl. Phys. Lett.* **82** (1999) 55.
3. J. Heikenfeld, M. Garter, D.S. Lee, R. Birkhahn, and A.J. Steckl, *Appl. Phys. Lett.* **75** (1999) 1189.
4. A.J. Steckl, M. Garter, D.S. Lee, J. Heikenfeld, and R. Birkhahn, *Appl. Phys. Lett.* **75** (1999) 2184.
5. J.B. Gruber, B. Zandi, H.J. Lozykowski, and W.M. Jadwiszczak, *J. Appl. Phys.* **91** (2002) 2929.
6. T. Monterio *et al.*, *Phys. B* **308** (2001) 22.
7. J.T. Torvik, R.J. Feuerstein, C.H. Qiu, J.I. Pankove, and F. Nammavar, *J. Appl. Phys.* **82** (1997) 1824.
8. J. Heikenfeld and A.J. Steckl, *Appl. Phys. Lett.* **77** (2000) 3520.
9. J.M. Zavada *et al.*, *Mat. Sci. Eng. B* **81** (2001) 127.
10. S. Kim *et al.*, *Appl. Phys. Lett.* **71** (1997) 231.
11. H.J. Lozykowski, *Phys. Rev. B* **48** (1993) 17758.